

Supplementary Information

Novel non-helical antimicrobial peptides insert into and fuse lipid model membranes

Saheli Mitra¹, Bhairavi Chandarsekhar¹, Yunshu Li¹, Mark Coopershlyak¹, Margot E. Mahoney¹, Brandt Evans¹, Rachel Koenig¹, Stephen C. L. Hall², Beate Klösgen³, Frank Heinrich^{1,4}, Berthony Deslouches⁵,
Stephanie Tristram-Nagle^{1*}

¹Biological Physics Group, Physics Department, Carnegie Mellon University, Pittsburgh, PA 15213, USA;

²ISIS Neutron and Muon Source, Rutherford Appleton Laboratory, Harwell Campus, Didcot, Oxfordshire,

OX11 0QX, UK; ³University of Southern Denmark, Dept. Physics, Chemistry & Pharmacy, PhyLife,

Campusvej 55, ODENSE M 5230, Denmark; ⁴Center for Neutron Research, National Institute of Standards

and Technology, Gaithersburg, MD 20899, USA; ⁵Department of Environmental and Occupational Health, University of Pittsburgh, Pittsburgh, PA 15261, USA

*Corresponding author's email: stn@cmu.edu

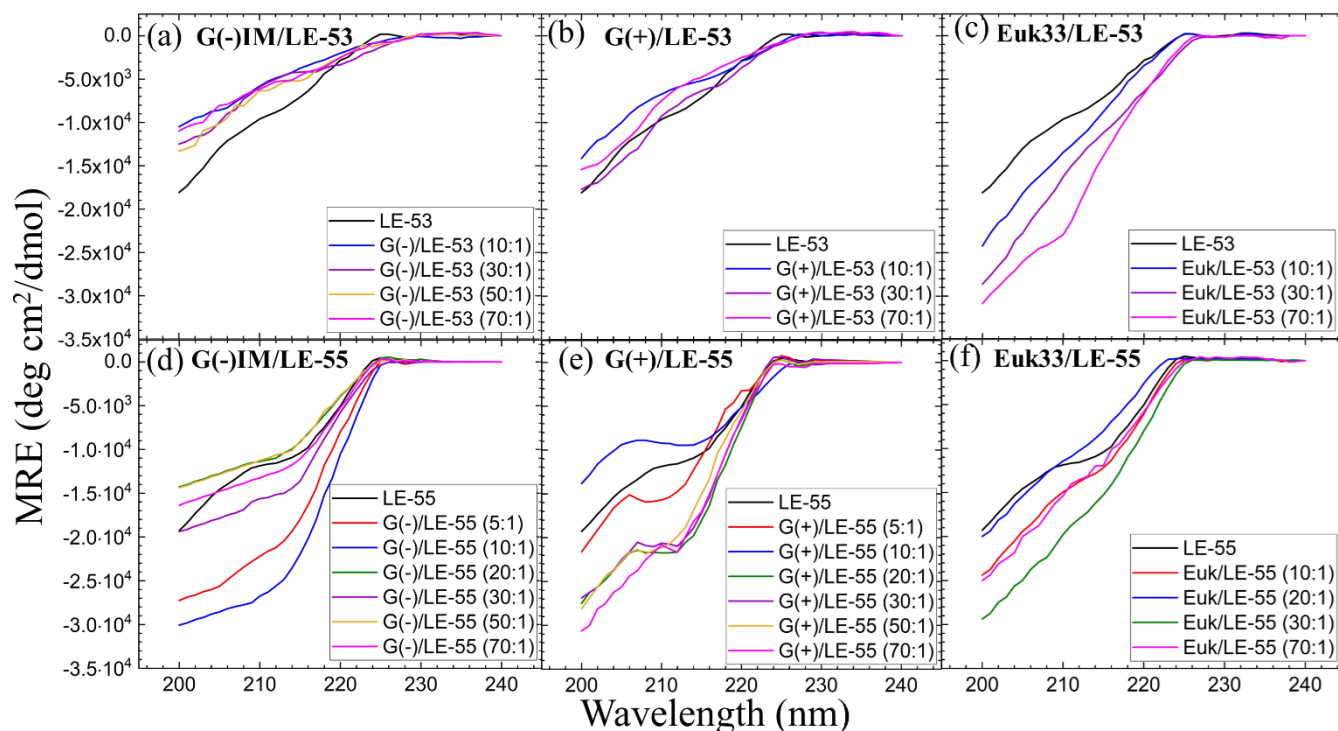


Fig. S1 MRE results of LE-53 (a, b and c) and LE-55 (d, e and f) in G(-)IM, G(+), and Euk33 LMM ULVs.

Tables S1 – S6 summarize secondary structural results (% α -helix, β -sheet, β -turn and random coil) for LE-53 and LE-55 peptides in three LMMs. R^2 indicates the goodness of fit. Std. devs. were generally ~5-7 % of the values shown.

Table S1. LE-53 CD results of secondary structure in G(-) IM LMMs

G(-) IM/LE-53	α-helix (%)	β-sheet (%)	β-turn (%)	Random	R^2
0:1	0 \pm 0	38.9 \pm 1.1	0 \pm 0	61.1 \pm 1.1	0.99
10:1	12.1 \pm 2.6	26.2 \pm 2.5	0 \pm 0	61.4 \pm 1.4	0.98
20:1	0 \pm 0	41.4 \pm 0.8	0 \pm 0	58.6 \pm 0.8	0.98
30:1	0 \pm 0	39.6 \pm 0.2	0 \pm 0	60.4 \pm 0.2	0.98
50:1	0 \pm 0	39.2 \pm 1.0	0 \pm 0	60.8 \pm 1.0	0.99

Table S2. LE-53 CD results of secondary structure in G(+) LMMs

G(+)/LE-53	α-helix (%)	β-sheet (%)	β-turn (%)	Random	R^2
0:1	0 \pm 0	41.1 \pm 0.5	0 \pm 0	58.9 \pm 0.5	0.99
10:1	0 \pm 0	41.7 \pm 0.4	0 \pm 0	58.3 \pm 0.4	0.99
30:1	0 \pm 0	41.0 \pm 0.4	0 \pm 0	59.0 \pm 0.4	0.99
70:1	0 \pm 0	39.3 \pm 0.6	0 \pm 0	60.7 \pm 0.6	0.99

Table S3. LE-53 CD results of secondary structure in Euk33 LMMs

Euk33/LE-53	α-helix (%)	β-sheet (%)	β-turn (%)	Random	R^2
0:1	0 \pm 0	41.1 \pm 0.5	0 \pm 0	58.9 \pm 0.5	0.99
10:1	0 \pm 0	40.4 \pm 1.4	0 \pm 0	59.6 \pm 1.4	0.99
30:1	0 \pm 0	40.9 \pm 0.0	0 \pm 0	59.4 \pm 0.4	0.99
70:1	0 \pm 0	42.9 \pm 0.7	0 \pm 0	57.1 \pm 0.7	0.99

Table S4. LE-55 CD results of secondary structure in G(-) IM LMMs

G(-) IM/LE-55	α-helix (%)	β-sheet (%)	β-turn (%)	Random	R²
0:1	0 \pm 0	43.5 \pm 1.5	0 \pm 0	56.5 \pm 1.5	0.96
5:1	0 \pm 0	45.0 \pm 0.1	0 \pm 0	55.0 \pm 0.1	0.97
10:1	0 \pm 0	46.2 \pm 0.3	0 \pm 0	53.8 \pm 0.3	0.94
20:1	0 \pm 0	43.5 \pm 3.0	0 \pm 0	56.5 \pm 3.0	0.98
30:1	0 \pm 0	45.7 \pm 1.9	0 \pm 0	54.3 \pm 1.9	0.97
50:1	0 \pm 0	45.4 \pm 1.8	0 \pm 0	54.6 \pm 1.8	0.97
70:1	0 \pm 0	45.3 \pm 0.4	0 \pm 0	54.7 \pm 0.4	0.96

Table S5. LE-55 CD results of secondary structure in G(+) LMMs

G(+)/LE-55	α-helix (%)	β-sheet (%)	β-turn (%)	Random	R²
0:1	0 \pm 0	43.5 \pm 1.5	0 \pm 0	56.5 \pm 1.5	0.96
5:1	0 \pm 0	41.8 \pm 1.2	0 \pm 0	58.2 \pm 1.2	0.98
10:1	0 \pm 0	43.3 \pm 0.9	0 \pm 0	56.7 \pm 0.9	0.99
20:1	0 \pm 0	43.4 \pm 1.2	0 \pm 0	56.6 \pm 1.2	0.96
30:1	0 \pm 0	42.7 \pm 0.2	0 \pm 0	57.3 \pm 0.2	0.98
50:1	0 \pm 0	42.9 \pm 1.5	0 \pm 0	57.2 \pm 1.5	0.97
70:1	0 \pm 0	42.5 \pm 1.0	0 \pm 0	57.5 \pm 1.0	0.97

Table S6. LE-55 CD results of secondary structure in Euk33 LMMs

Euk33/LE-55	α-helix (%)	β-sheet (%)	β-turn (%)	Random	R²
0:1	0 \pm 0	43.5 \pm 1.5	0 \pm 0	56.5 \pm 1.5	0.96
10:1	0 \pm 0	44.1 \pm 1.6	0 \pm 0	55.9 \pm 1.6	0.99
20:1	0 \pm 0	43.1 \pm 2.5	0 \pm 0	56.9 \pm 2.5	0.99
30:1	0 \pm 0	44.9 \pm 1.8	0 \pm 0	55.1 \pm 1.8	0.99
70:1	0 \pm 0	44.0 \pm 1.1	0 \pm 0	56.0 \pm 1.1	0.99

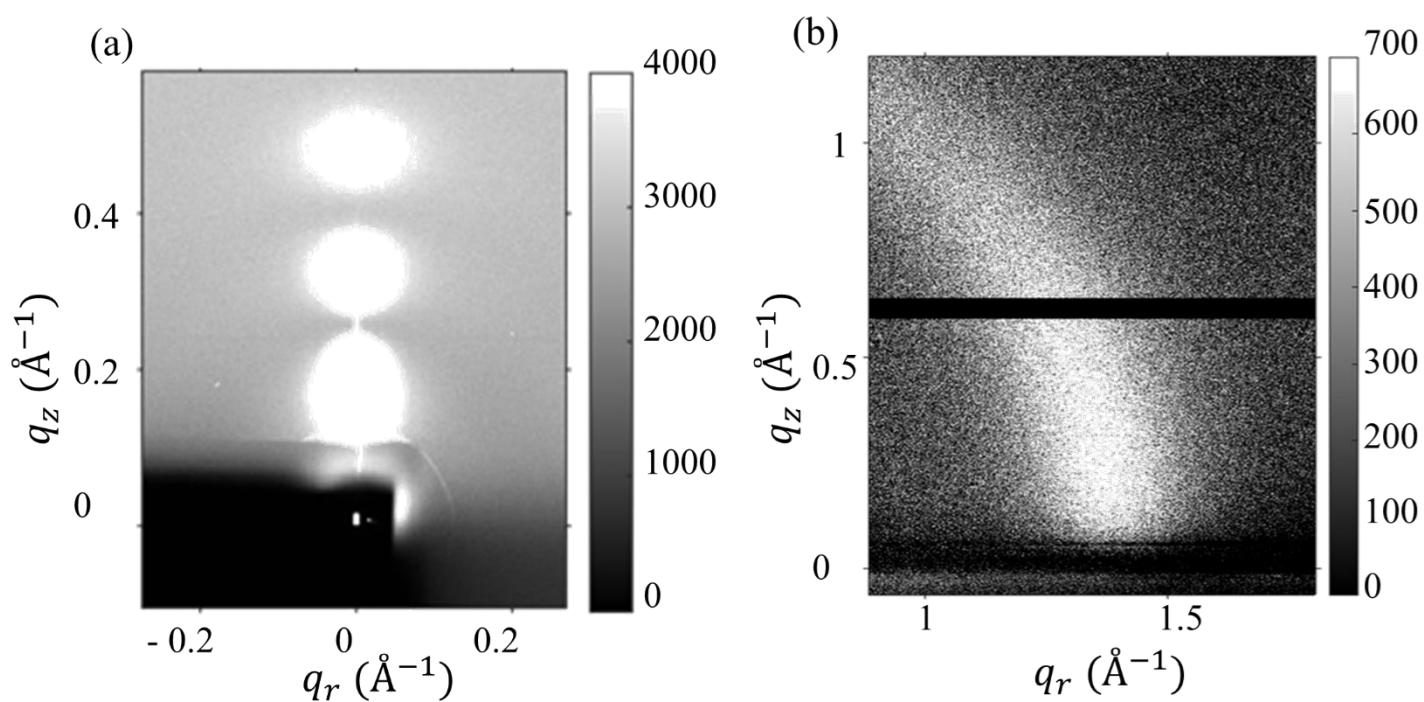


Fig. S2 XDS data obtained at CHESS. Results of 250:1 G(-)IM/LE-53 at 37 °C. **(a)** Low angle x-ray scattering (LAXS). The sample is fully hydrated with a D-spacing of 102 Å. Three lobes of diffuse x-ray scattering result from fluctuations in the oriented stack of membranes at high hydration. **(b)** Wide angle x-ray scattering (WAXS). The chain correlation is the intensity centered at $q_r \cong 1.4 \text{ \AA}^{-1}$ which corresponds to $\cong 4.5 \text{ \AA}$ d-spacing. Light grey indicates positive intensity values (see color bars). Black line contains no intensity information and was removed during data analysis.

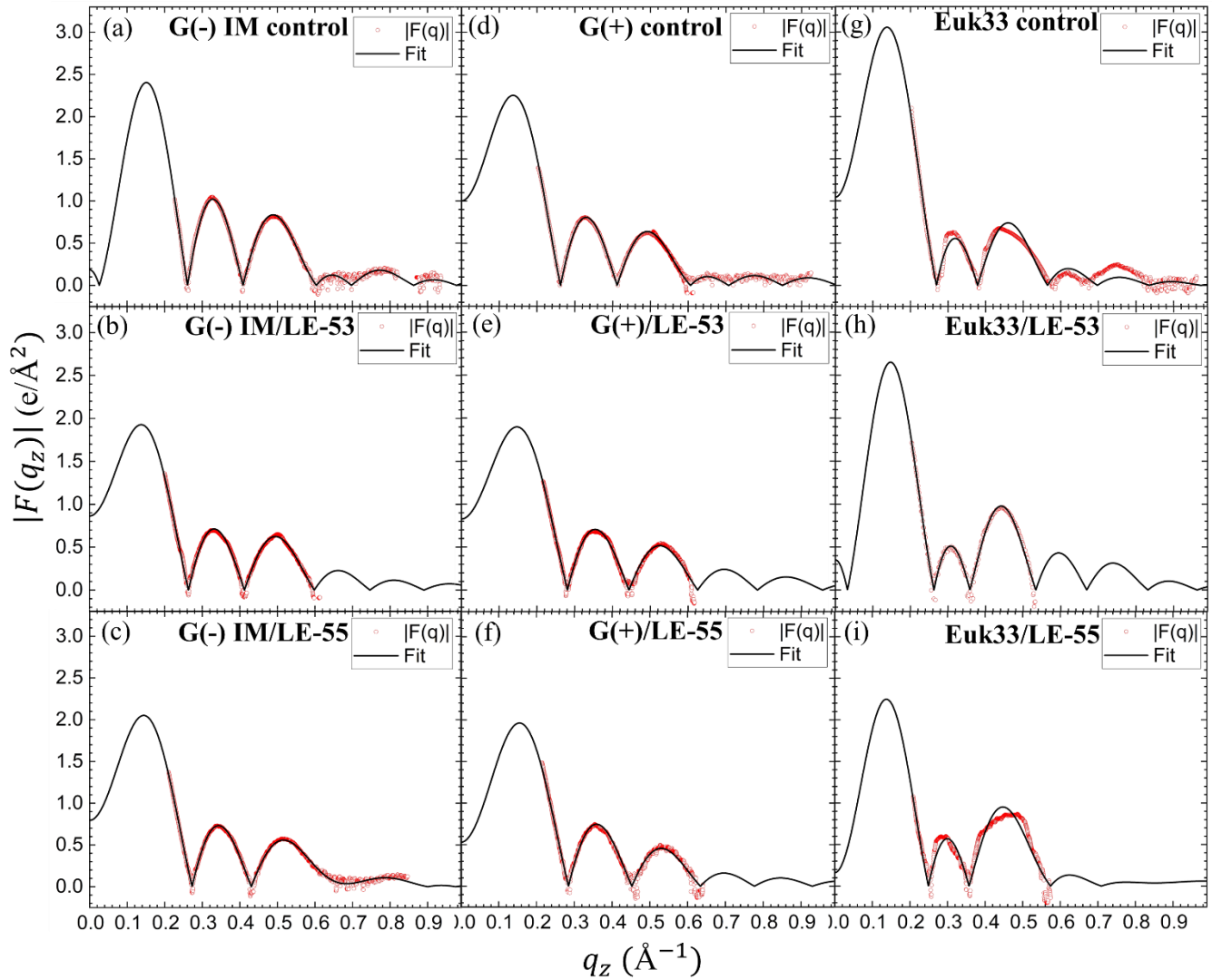


Fig. S3 $|F(q_z)|$ for G(-) IM LMMs (a – c), G(+) LMMs (d - f) and Euk33 LMMs (g - i) in the presence of LE-53 and LE-55. The red points are experimental data, and the black line is the SDP model fit to the data. Lipid/peptide molar ratio is 75:1.

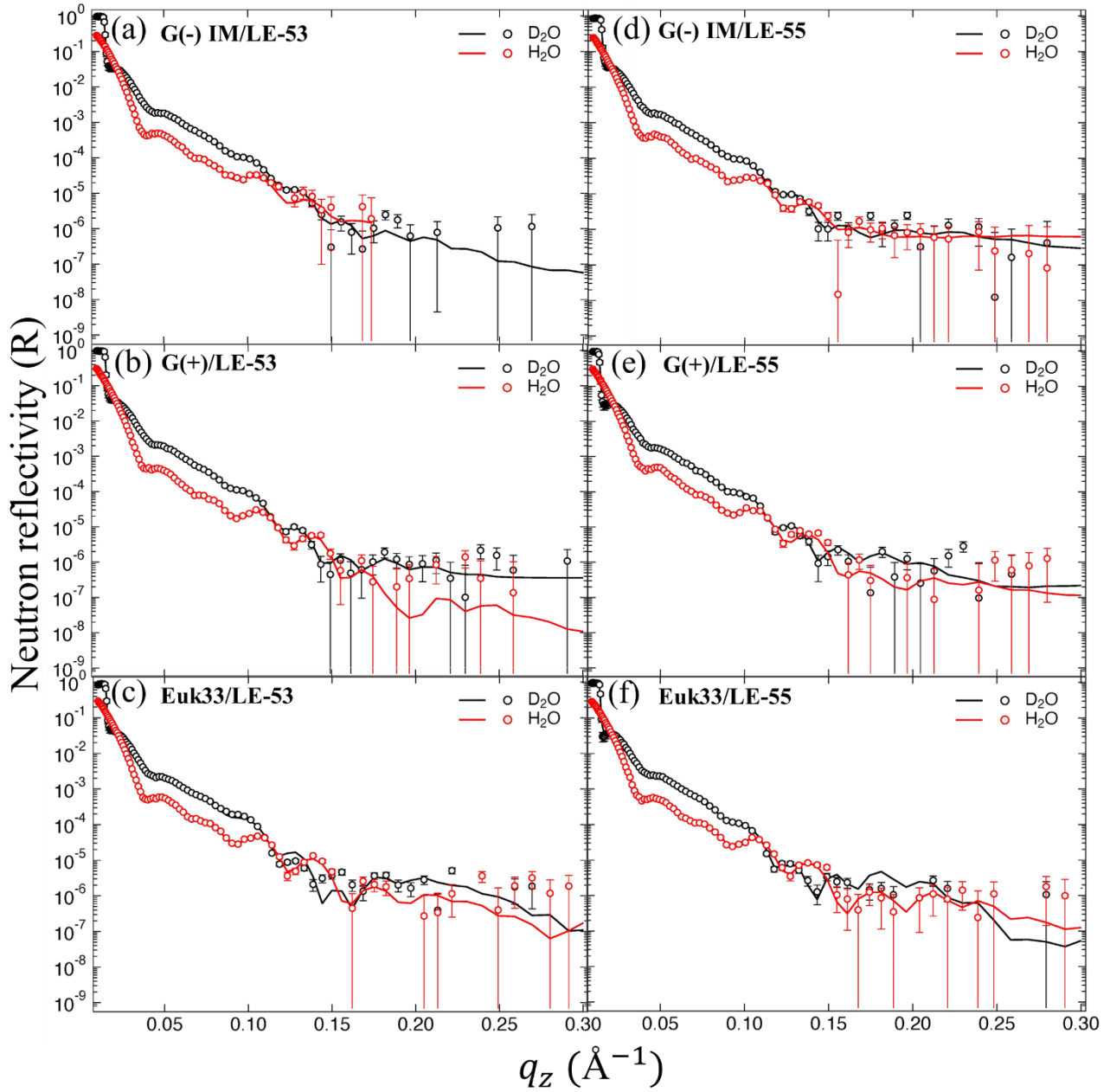


Fig. S4 Neutron reflectivity scattering length profiles of G(-) IM LMMs (**a and d**), G(+) LMMs (**b and e**) and Euk33 LMMs (**c and f**) in the presence of LE-53 and LE-55. The solid black and red lines are the fits to the D₂O and H₂O data respectively.

Table S7. NR results of LE-53 and LE-55 in G(-)IM, G(+) and Euk33 LMMs.

Parameter	G(-)/LE-53	G(+)/LE-53	G(-)/LE-55	G(+)/LE-55	Euk33 LE-53	Euk33 LE-55
Substrate						
SiOx nSLD / 10^{-6} \AA^{-2}	3.2 ± 0.2	3.3 ± 0.2	3.3 ± 0.1	3.3 ± 0.2	3.2 ± 0.1	3.2 ± 0.1
SiOx thickness / \AA	24 ± 13	21 ± 12	24 ± 11	25 ± 15	25 ± 14	25 ± 14
Cr nSLD / 10^{-6} \AA^{-2}	3.3 ± 0.4	3.1 ± 0.2	3.3 ± 0.3	3.3 ± 0.5	3.3 ± 0.4	3.2 ± 0.4
Cr thickness / \AA	26 ± 9	26 ± 11	24 ± 9	24 ± 9	26 ± 12	25 ± 11
Au nSLD / 10^{-6} \AA^{-2}	4.5 ± 0.1	4.4 ± 0.1	4.52 ± 0.09	4.67 ± 0.07	4.65 ± 0.09	4.5 ± 0.1
Au thickness / \AA	168 ± 6	169 ± 3	169 ± 4	169 ± 5	171 ± 3	168 ± 5
R.M.S. roughness / \AA	8 ± 2	8 ± 1	9 ± 2	7 ± 1	2.4 ± 0.3	4 ± 1
Bilayer						
R.M.S. roughness / \AA	5 ± 1	7 ± 1	6 ± 1	7 ± 2	2.6 ± 0.5	4 ± 1
Tether thickness / \AA	10 ± 2	10 ± 2	9 ± 2	10 ± 2	10 ± 1	10 ± 2
Hydrocarbon thickness inner lipid leaflet / \AA	16 ± 4	19 ± 3	17 ± 4	18 ± 3	19 ± 3	19 ± 3
Hydrocarbon thickness outer lipid leaflet / \AA	16 ± 4	14 ± 3	17 ± 4	14 ± 3	16 ± 4	15 ± 3
Area per lipid, outer leaflet / \AA^2	70 ± 20	90 ± 20	70 ± 20	80 ± 20	60 ± 10	60 ± 10
Bilayer completeness / %	90 ± 8	94 ± 5	92 ± 6	92 ± 6	97 ± 3	98 ± 2
Peptide						
Amount of membrane-associated protein / $\text{\AA}^3/\text{\AA}^2$	6 ± 3	4 ± 2	5 ± 2	5 ± 2	2 ± 1	3 ± 1
Fraction of protein in hydrocarbons	0.51 ± 0.18	0.70 ± 0.13	0.62 ± 0.12	0.66 ± 0.13	0.80 ± 0.18	0.68 ± 0.16
Fraction of protein in headgroups	0.24 ± 0.08	0.23 ± 0.08	0.23 ± 0.07	0.24 ± 0.06	0.17 ± 0.16	0.24 ± 0.12
Fraction of protein in bulk solvent	0.19 ± 0.14	0.04 ± 0.04	0.10 ± 0.08	0.05 ± 0.04	0.02 ± 0.02	0.02 ± 0.02
Peak position from headgroup / solvent interface / \AA	-16 ± 6	-14 ± 4	-13 ± 5	-13 ± 3	-23 ± 11	-16 ± 6
General						
Goodness of fit, chi-squared	1.4	0.9	1.3	2.2	4.0	2.4

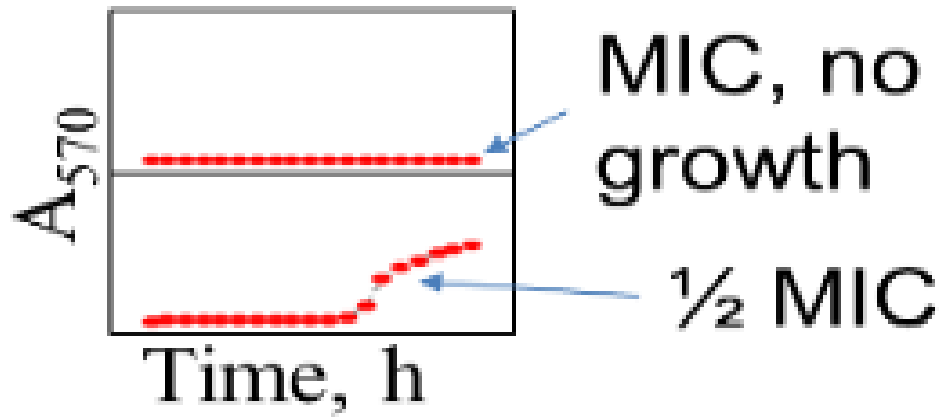


Fig. S5 Assessment of MIC: using a plate reader bacterial turbidity is detected every hour, represented by a red dot, for 18 hours. The growth kinetics, shown as a flat line moved higher, indicate no bacterial growth. The lowest concentration corresponding to a flat growth kinetics line is the MIC or minimum inhibitory concentration.